ACS APPLIED MATERIALS & INTERFACES

Research Article

www.acsami.org

Characterization, Antimicrobial Activities, and Biocompatibility of Organically Modified Clays and Their Nanocomposites with Polyurethane

Ming-Chien Wang,[†] Jiang-Jen Lin,[‡] Hsiang-Jung Tseng,[†] and Shan-hui Hsu*[,‡,§]

[†]Department of Chemical Engineering, National Chung Hsing University, Taichung, 40227 Taiwan, R.O.C.

[‡]Institute of Polymer Science and Engineering and [§]Rehabilitation Engineering Research Center, National Taiwan University, Taipei, 10617 Taiwan, R.O.C.

ABSTRACT: A novel method to exfoliate the montmorillonite clay was developed previously to generate random nanosilicate platelets (NSP), one kind of delaminated clay. To improve their dispersion in a polymer, we modified NSPs by three types of surfactants (cationic Qa, nonionic Qb, and anionic Qc) in this study and used them to prepare nanocomposites with polyurethane (PU). The zeta potential, antimicrobial ability, and biocompatibility of these surfactant-modified NSPs (abbreviated "NSQ") were characterized. It was found that the zeta potential of Qa-modified NSP (NSQa) was positive, whereas those of NSP and the other two NSQs (NSQb and NSQc) were negative. All NSQ presented less cytotoxicity than NSP. NSQa and NSQc showed excellent antimicrobial activities against *S. aureus* (Gram-positive strain) and *E. coli* (Gram-negative strain). The nanocomposites of NSQ with PU were then characterized for surface and mechanical properties, cell attachment and proliferation, antimicrobial activity in vitro, and biocompatibility in vivo. A higher surfactant to NSP ratio was found to improve the dispersion of NSQ in PU matrix. The mechanical properties of all PU/NSQ nanocomposites were significantly enhanced. Among various NSQ, only NSQa were observed to migrate to the composite surface. The attachment and proliferation of endothelial cells and fibroblasts in vitro as well as biocompatibility in vivo were significantly better for PU/NSQa containing 1% of NSQa than other materials. The microbiostasis ratios of PU/NSQ nanocomposites containing 1% NSQa or NSQc were >90%. These results proposed the safety and potential antimicrobial applications of surfactant-modified delaminated clays and their nanocomposites with PU polymer.

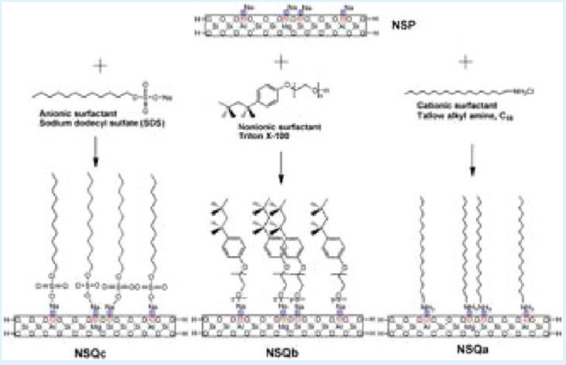

KEYWORDS: *clay, antimicrobial, polyurethane, biocompatibility, nanocomposite*

1. INTRODUCTION

The microstructure of a polymer and its physicochemical properties can be manipulated by making composites. The composites with nanomaterials,[1−3] especially those containing clay or layered silicates, have attracted much attention because of their availability at a relatively low cost.[3−5] Preparation for polymer nanocomposites with clay from solution usually requires water and a cosolvent (e.g., chloroform, xylene, or other organic solvents). Intercalation only occurs in certain polymer/clay pairs using this method.[4,5] Delaminated clay exfoliated from the natural sodium montmorillonite clay by a novel one-step process has been previously developed.[6,7] Such delaminated clay, so-called nanosilicate platelets (NSP), can be resuspended in water and self-assemble into microscale fiber bundles after water evaporation.[8] The individual platelets possess high aspect ratio and strong face-to-face ionic character and thus may inhibit bacterial growth as a result of "physical trapping".[9] Unfortunately, NSP are dispersed only in water, but most polymers are hydrophobic. The direct interaction of NSP with mammalian cell membrane also leads to a certain extent of cytotoxicity. The dispersion of NSP in organic solvents may be achieved by capping NSP with a cationic or nonionic surfactant.[10] When these surfactant-modified NSP (or "NSQ") are mixed in a polymer matrix, they are expected to remain exfoliated in the polymer matrix. Because the clay content required for an exfoliated nanocomposite is usually lower than that for an intercalated nanocomposite,[5] the composites of NSQ with a polymer could have some attractive properties. Moreover, surfactant-capped nanomaterials are known to protect the cells from the direct contact with the nanomaterials and reduce the associated cytotoxicity.[11]

Polyurethane (PU) polymers have microphase separation arising from the thermodynamic incompatibility between their soft and hard segments. They have wide ranges of physical and chemical properties[12] and are used in cardiovascular or other biomedical devices because of the good biocompatibility.[13−15]

Received: October 14, 2011
Accepted: November 30, 2011
Published: November 30, 2011

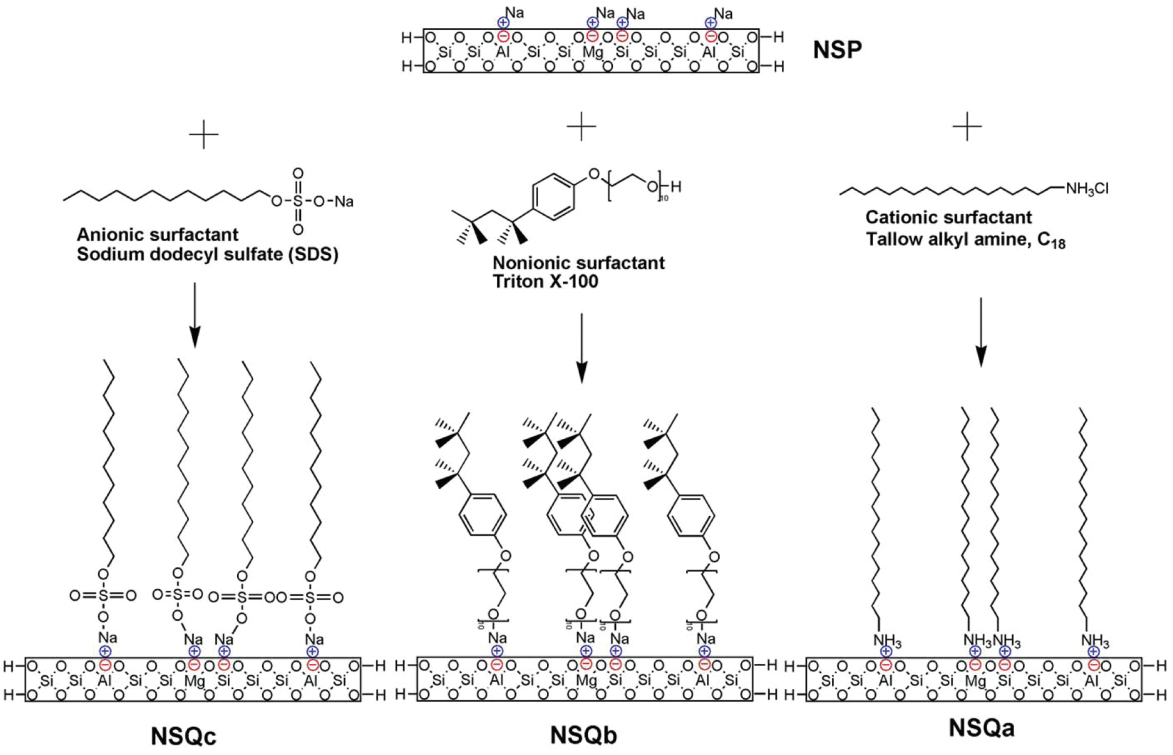

Figure 1. Chemical compositions of exfoliated clay NSP and those modified by various surfactants (NSQ).

The nanocomposites of PU can especially own interesting features when the characteristic size of phase separation and that of the filled nanomaterials are similar.[16] Organic compounds including chlorhexidine diacetate and quaternary ammonium compounds have been used to modify clays and to mix them in PU and other polymers.[17,18] These organic compounds usually have cytotoxicity and health concerns. Even though organically modified silicates and their polymer nanocomposites can have excellent antimicrobial activity,[19,20] the inferior biocompatibility may prevent them from biomedical applications. Using relatively safe surfactants in low concentrations may be more appropriate when these nanocomposites are intended to be used in vivo.

In this study, we developed three different organically modified clays (NSQ) each using a cationic, nonionic, and anionic surfactant and determined their surface charge, cytotoxicity and antimicrobial efficacy. Moreover, nanocomposites from a commercial biomedical PU (Pellethane) and various concentrations of NSQ were prepared (abbreviated as PU/NSQ). The microstructure of PU/NSQ were characterized by the transmission electron microscopy (TEM), atomic force microscopy (AFM), field emission scanning electron microscopy (FESEM), attenuated total reflectance infrared (ATR-IR) spectroscopy, contact angle, and dynamic mechanical analysis (DMA). The attachment and proliferation of endothelial cells (ECs) and fibroblasts on the surface of the materials were evaluated. The antimicrobial efficacy as well as the in vivo biocompatibility of the nanocomposites was further analyzed in order to assess their potentials for biomedical applications.

2. EXPERIMENTAL SECTION

2.1. Preparation of Delaminated Clays NSP and NSQ. NSP were isolated by the one-step exfoliation process of natural sodium montmorillonite clay and toluene/aqueous NaOH extraction.[8,9] In this process, the pristine sodium montmorillonite was intercalated with polyamine, and the layered silicates of montmorillonite were exfoliated. The polyamine on the exfoliated silicates was extracted by NaOH, H_2O, and toluene to render the individually suspended nanosilicate platelets (i.e., NSP). Each NSP surface was occupied by 18 000 sodium ions to form the repulsive force that made them stably dispersed in water. The basal spacing of the pristine sodium montmorillonite was 1.24 nm, and that of NSP was increased to be featureless in XRD pattern.[21] The dimension of each platelet was approximately 80 × 80 × 1 nm (length × width × height). From NSP, three types of NSQ (NSQa, NSQb, and NSQc) were prepared by the use of different surfactants, as illustrated in Figure 1. Each of them was modified from NSP by a cationic, nonionic or anionic surfactant. To prepare NSQa, 10 wt % NSP in water suspension (30 g) was added with 10 wt % *n*-octadecanylamine hydrochloride salt (n-$C_{18}H_{37}NH_3^+$, cationic surfactant Qa) in water suspension (70 g) in a round-bottomed flask equipped with a magnetic stirrer. The solution was heated to 80 °C for 1 h. Because of the strong interaction between NSP and C18-fatty amine, the percentage of NSQa, i.e., NSP complexed with the fatty amine (the efficiency of capping), was over 99% after 1 h of treatment.[10] NSQb were prepared using Triton X-100 (a nonionic surfactant Qb). The weight ratio of NSP to Triton X-100 is 30/70. To prepare NSQb, 10 wt % NSP in water slurry (100 g) was added with Triton X-100 (23.5 g) in a round-bottomed flask. The slurry was agitated by a magnetic stirrer to form gelled products (NSQb) and then were collected and subjected to freeze-drying.[22] The preparative procedure of NSQc was similar to that of NSQb, except that the surfactant was replaced by sodium dodecyl sulfate (SDS, an anionic surfactant Qc). On the basis of the above procedures, each NSQ contained 70% surfactant and 30% NSP.

All delaminated clays including NSP and NSQ (0.1 wt %) were measured for their zeta potential in double deionized water (DDW). Delsa Nano S (Beckman Coulter, USA), a zeta potential and submicrometer particle size analyzer, was used to determine the zeta potential of NSP and NSQ.

2.2. Cytotoxicity Tests of NSP and NSQ. L929 mouse fibroblasts purchased from the American Type Culture Collection (ATCC) were cultured in 10 mL of low glucose Dulbecco's Modified Eagle's Medium (DMEM, Gibco, USA) containing antibiotics (100 U/ml penicillin G and 100 μg/mL streptomycin) and 10% fetal bovine

dx.doi.org/10.1021/am2014103 | ACS Appl. Mater. Interfaces 2012, 4, 338–350

serum (FBS) in a 5% CO_2 incubator at 37 °C. After 2 to 3 days, nearly confluent cultured cells were trypsinized using 0.05% trypsin-EDTA solution and were passaged to T75 flasks. L929 were cultured in 24-well tissue culture plates (Corning, USA) and each well was injected 1 mL of cell suspension containing 1×10^5 cells. Cells cultured in the medium were used as the negative control and that in the medium containing 5.0% dimethyl sulfoxide (DMSO, Sigma, USA) were used as the positive control. After 24 h, the medium was removed from each well and washed twice with phosphate buffered saline (PBS). The nearly confluent cell monolayer was challenged by 1 mL of medium containing 10 ppm NSP or NSQ for 24 h. After that, the medium was again removed and washed twice with PBS to eliminate free cells. MTT assay was used to determine the viability of adherent cells. Briefly, 300 μL of 3-(4,5-dimethylthiazol-2-yl)-2,5-diphenyltetrazolium bromide (MTT) (Sigma, USA) solution (0.5 mg/mL, 1× PBS) was added and incubated at 37 °C in the dark. After 4 h, the supernatant was removed and 600 μL of DMSO (Tedia, Fairfield, OH, USA) was added into each well to dissolve the resulting formazan crystals in 10 min. A microplate reader (DV-990-BV, Italy) was used to determine the optical density (OD) values at wavelength 550 nm, which represented cell viability on the surface of each sample.

2.3. Antimicrobial Tests of NSP and NSQ. *Staphylococcus aureus* (*S. aureus*) and *Escherichia coli* (*E. coli*) were used as the Gram-positive and Gram-negative strains for evaluation of the antimicrobial activities. To avoid possible bias from the testing protocols, we used three methods with different protocols, including the agar diffusion method, halo zone method, and direct contact method.[23] The nutrient broth comprised of peptone (Himedia, India), beef extract (Himedia, India) and NaCl (Sigma, USA) dissolved in DDW and sterilized by an autoclave at 103 kPa for 20 min. The broth was used to culture bacteria and to adjust the appropriate number of bacterial colony forming units (CFU) for experiments. Eight and a half grams of sodium chloride (Sigma, USA) and 0.0425 g of potassium dihydrogen phosphate (Sigma, USA) were dissolved in 1 L of distilled water and served as the buffer solution. The nutrient agar was prepared from broth containing 1.5% agar [Becton, Dickinson and Company (BD), USA] and the pH was adjusted between 7.0 and 7.2. The agar and buffer solution were autoclaved for 20 min. As the temperature of the agar solution temperature was cooled to 45 °C, a certain amount (about 15 mL) was poured into each of a 100 mm diameter Petri dish and cooled again to room temperature for the use in the agar diffusion method and direct contact method.

In the agar diffusion method, 100 μL of the broth with 1×10^6 *S. aureus* or *E. coli* were spread throughout each agar plate. The concentrations for testing included 0.1% and 1.0% of nano silicates. One-hundred micorliters of the nanosilicate aqueous suspension were adsorbed on each paper disk (10 mm in diameter) that was placed on each of the inoculated agar. The nanosilicates produced inhibition zone around the paper discs, of which the width was measured at 37 °C after 24 h.

In the halo zone method, the concentration of bacterial suspension was adjusted to 1.5×10^8 CFU/mL. The sterilized melt culture agar in 150 mL was mixed with 1.5 mL of bacterial suspension. The mixture was poured into Petri dishes and solidified under room temperature. In each dish three wells were drilled and filled with 40 μL of the nanosilicate aqueous suspension. These dishes were then incubated at 37 °C. The diameters of the inhibition zone were measured after 24 h.

In the direct contact method, the pure nutrient broth was diluted by the buffer solution (in 1:400). The number of *S. aureus* and *E. coli* in the inoculum was 4×10^5/mL in the diluted nutrient broth for each sample. A proper amount of NSP or NSQ was added into each sample so the concentration of NSQ was 0.001, 0.01, and 0.1 wt % in solution. Samples were cultured and shaken at 110 rpm and 35 °C. After 24 h, 1 mL of the sample was spread on the nutrient agar in Petri dish. The nutrient agar and bacteria in the dish were incubated at 37 °C for 24 h and the CFU was counted.

2.4. Preparation and Characterization of PU/NSQ Nanocomposites. The commercial biomedical grade PU, Pellethane 2363−80A (Upjohn, USA), was used. This polymer was synthesized based on 4,4′-diphenylmethane diisocyanate (as the hard segment), polytetramethylene oxide (as the soft segment) and 1,4 butanedioal (as the chain extender). One gram of PU and NSQ were each dissolved in the dimethylacetamide (DMAc) solvent (100 mL) and agitated for 24 h. NSQ/DMAc suspension was added in PU solution at different ratios, so the concentration of NSQ in the final polymer composite was 0.01, 0.1, 1.0, and 5.0% (abbreviated as PU/NSQ 5% and so on). The mixture was agitated for another 24 h. The solution was cast on 15 mm diameter coverslip glass or on 6 cm glass dish. The cast nanocomposites ("PU/NSQ") were placed in an oven at 60 °C for 24 h and then in vacuum for 48 h to remove the residual solvent.

For TEM, 1 wt % solution of PU/NSQ solution was cast onto copper grids, dried at 60 °C for 24 h, followed by further drying in the vacuum oven at 60 °C for 48 h to remove the residual solvent. The specimens were examined by a transmission electron microscope (JEOL JEM-1200, Japan) operated at 110 kV.

The surface morphology of all PU/NSQ films was examined by a FESEM (JEOL JSM-7401F, Japan) and AFM (CP−II, Veeco, USA). The energy-dispersive spectrometry (EDS) was used to determine the chemical composition. Topography and phase images of AFM were recorded simultaneously in tapping mode with a cantilever (spring constant 20−75 N/m) coated with Al on the reflective side (NSC 15/AIBS/50, MikroMasch, USA). The maximum height, root-mean-square roughness, average roughness and mean height of samples were calculated within the given area by computer software (Image processing ver.2.0, Veeco, USA). The surface chemistry was analyzed by the attenuated total reflectance infrared spectroscopy (ATR-IR) in the spectral region of 4000−600 cm^{-1} by a Fourier Transformed infrared spectrometer (Spectrum One, Perkin-Elmer, USA). The water contact angle of the surface was measured by a contact angle meter (First Ten Angstrom, FTA-125, USA) at 25 °C and 70% relative humidity. At least three readings were made on each sample and the values from at least three samples were averaged.

DMA was performed at a frequency of 1 Hz by a dynamic mechanical analyzer (DMA Q800, TA Instruments, USA). The temperature range was from −100 to 150 °C and the heating rate was 5 °C/min. The glass transition temperature (Tg) of the sample was defined as the temperature where the loss tangent (tan δ) reached a maximum. The dynamic modulus (the storage modulus E' and the loss modulus E'') were recorded. The static tensile properties of the materials were measured by a universal testing machine (Gotech Inc. AI-3000, Taiwan) at the testing speed of 100 mm/min at room temperature. The sample was rectangular in shape and the size was 56.0 mm × 5 mm.

2.5. Cell Attachment and Proliferation on PU/NSQ. Bovine carotid arterial endothelial cells (ECs) were harvested with the collagenase method. These cells can be cultured to higher passage numbers (e.g., 20) without appreciable loss of growth rate or phenotype. Cells between 10 to 20 passages were used in this study. The culturing procedures were the same as those of L929. PU/NSQ nanocomposites on 15 mm coverslip glass were sterilized by 75% ethanol, rinsed by PBS and placed into the bottom of each well in 24-well tissue culture plates (Corning, USA). Each well was injected 1 mL of cell suspension containing 2×10^4 cells. Cells cultured on the pure PU were used as the control. After 1 and 3 days, the medium was removed and the samples were washed twice with PBS to eliminate free cells. The viability of cells on the materials was determined by the MTT assay as previous described.

Human skin fibroblasts were purchased from Bioresource Collection and Research Center (Hsinchu, Taiwan). Cells between five to ten passages were used in this study. The culture medium was the minimum essential medium (MEM, Gibco, USA) containing antibiotics (100 U/ml penicillin G and 100 μg/mL streptomycin) and 10% FBS. The other experimental procedures followed those of ECs.

2.6. Antimicrobial Tests of PU/NSQ. The antimicrobial activities of PU/NSQ nanocomposites were evaluated following the JIS (Japanese Industrial Standard) Z2801 method. The PU/NSQ samples (5 cm ×5 cm) were sterilized by 75% ethanol and washed twice with DDW. The powders of peptone, beef extract and NaCl were dissolved in DDW as the culture broth, which was then sterilized by an autoclave at 103 kPa for 20 min. *S. aureus* and *E. coli* were

cultured in the broth for one day and the number of bacteria was adjusted to 1×10^6 CFU/mL. The inoculum (0.4 mL) was instilled on the surface of each sample. A square polyethylene film was used to cover the surface so the inoculum could be spread averagely. The other two groups of PU samples were set as the control groups, including the immediate and the tested groups. After inoculation, the immediate group of control was washed with 25 mL of SCDLP [soybean-casein digest broth (BD, USA) with lecithin and polysorbate (MP Biomedicals, USA)]. The plate count agar (PCA) contained 1.5% agar (BD, USA), the yeast extract (BD, USA), tryptone (BD, USA) and glucose (sigma, USA). The PCA was sterilized at 103 kPa for 20 min by an autoclave after the pH of PCA was adjusted to 6.8 to 7.2. One milliliter of bacterial SCDLP solution was cultured in 9 cm PCA Petri dish at 37 °C for 48 h and the CFU of the bacteria were counted. The tested group of control and the PU/NSQ samples inoculated with the test bacteria were incubated at a temperature of 35 °C and a relative humidity of ≥90% for 24 h. These samples were treated the same way as the immediate control to obtain the CFU of bacteria in 1 mL of SCDLP solution. The ratio of microbiostasis was defined by the following formula: [(CFU for the immediate group of control − CFU for the tested group of control or CFU for the samples)/CFU for the immediate group of control × 100%].

2.7. Biocompatibility of PU/NSQ In vivo. The nanocomposite films were cut to a uniform size (10 mm × 10 mm square, ∼0.2 mm thick), sterilized by 75% ethanol, rinsed, and placed in PBS. All animal procedures in this study were approved by the university Animal Care and Use Committee. Adult Sprague−Dawley rats (400−450 g) were anesthetized by isoflurane and an incision (∼10 mm × 10 mm) was created on each side of the dorsal. Sample films were inserted into the subcutaneous sites, one on each side. After 19 days, the rats were euthanized by CO_2 overdose treatment and all samples were explanted from the animals. For each PU/NSQ sample, several film specimens were washed by 1% Tween-20 surfactant solution in an ultrasonic bath for 5 min, rinsed thoroughly by DDW, and dried in an oven, before analyses by FESEM. A second group of specimens were washed slightly by PBS, fixed in 2.5% glutaraldehyde, dehydrated, and critical point dried before observation by FESEM. The third group of specimens were excised with surrounding tissue and fixed in 10% natural formalin solution, embedded in paraffin, thin-sectioned and stained by H&E for histological analysis under an optical microscope. The optical images were analyzed quantitatively by the Image Pro Plus 4.5 software. The average capsule thickness was evaluated in the thinnest parts of the foreign body fibrous capsule. Thinner fibrous capsules indicate good biocompatibility.

2.8. Statistical Analysis. The values from multiple samples were obtained, calculated and then expressed as mean ± standard deviation. The statistical significance of the samples was assessed by the method of single factor analysis of variance (ANOVA). p values less than 0.05 were considered significant.

3. RESULTS

The zeta potential of the unmodified delaminated clay, NSP, was about −43 mV. For the surfactant-modified delaminated clays, NSQa had positive (+42 mV) zeta potential while NSQb and NSQc remained negative (about −30 mV) zeta potential. The values of zeta potential confirmed the good stability of all nanomaterials when suspended in water.

The results of cytotoxic evaluation of NSP and various NSQ are shown in Figure 2. The viability of L929 fibroblasts in all groups of NSQ was close to the negative control and was significantly greater than the positive control, indicating little or

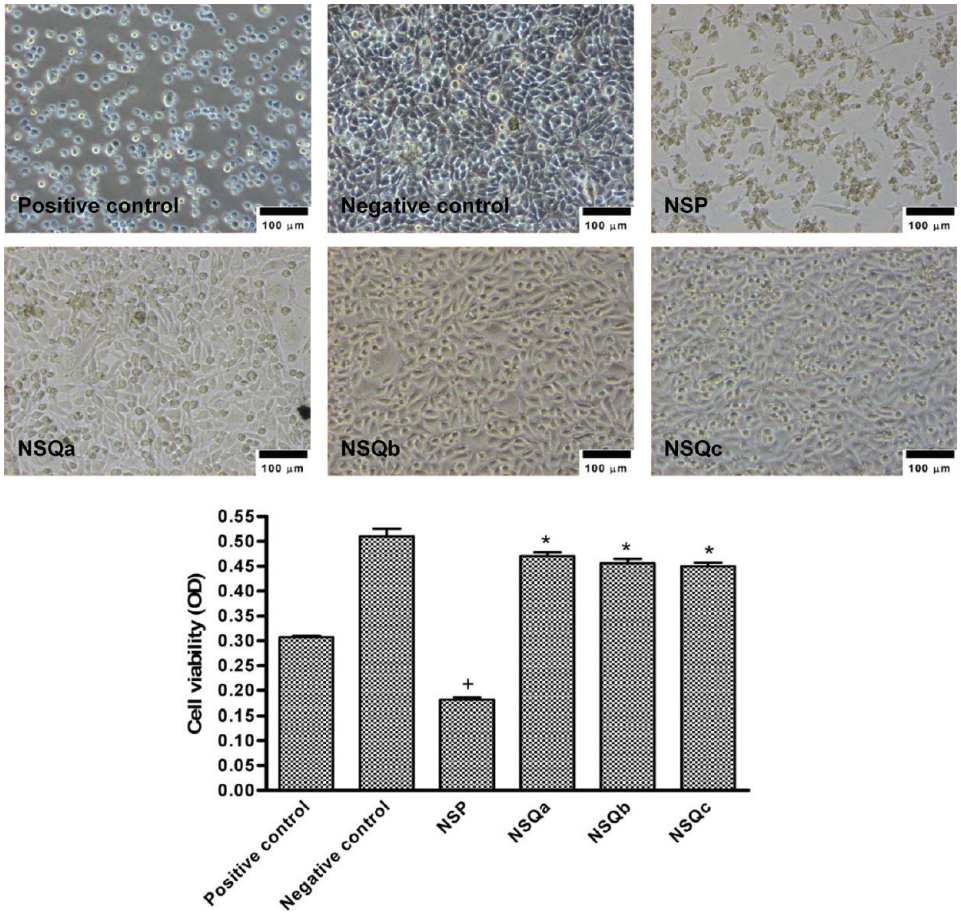

Figure 2. Cytotoxicity result for 10 ppm of NSP and NSQ. *, $p < 0.05$, significantly greater than positive control. +, $p < 0.05$, significantly lower than positive control.

dx.doi.org/10.1021/am2014103 | ACS Appl. Mater. Interfaces 2012, 4, 338−350

no toxicity. On the other hand, NSP at the same concentration (10 ppm) demonstrated cytotoxicity.

Figure 3 shows the antibacterial activities of NSP and various NSQ evaluated by the agar diffusion (Figure 3A), halo zone

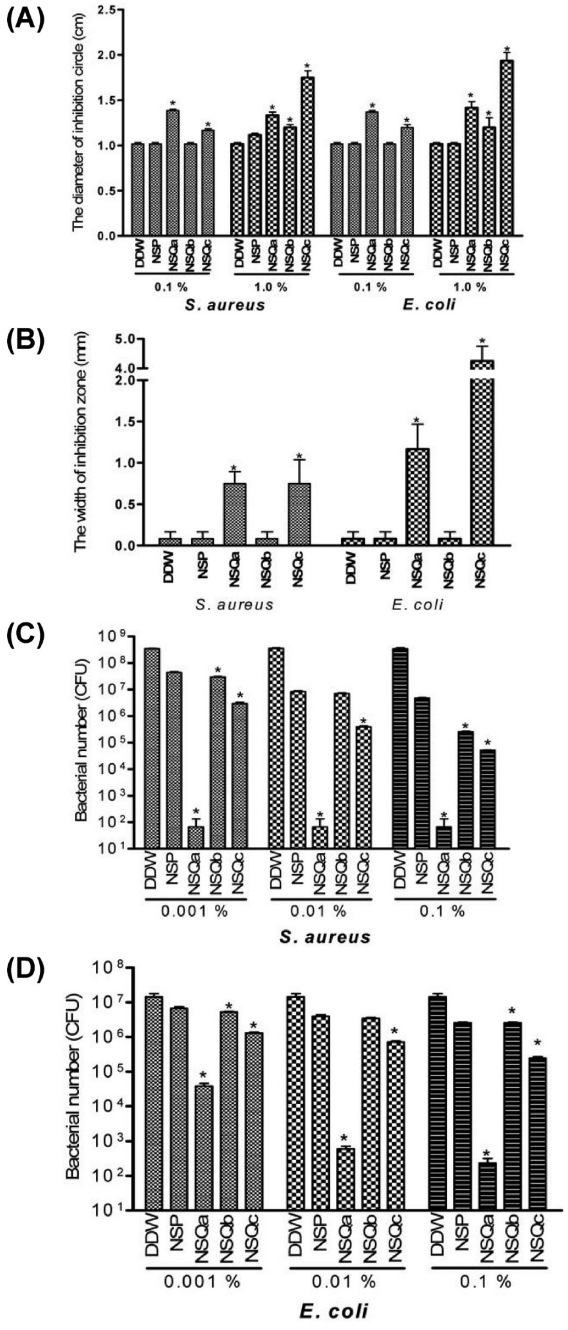

Figure 3. Antibacterial activity of NSP and NSQ by the (A) agar diffusion method, (B) halo zone method and (C, D) direct contact method. *, $p < 0.05$, significantly greater or lower than NSP.

(Figure 3B) or the direct contact method (Figure 3C, D). Similar results were obtained by the first two methods (Figure 3A, B), where the antibacterial activities against *S. aureus* and *E. coli* were the highest for NSQc, followed by NSQa, and the lowest for NSQb. Because the agar employed in these two testing methods may limit the diffusion of nanomaterials and influence the outcome, a third method based on the direct contact of the nanomaterials was used to assess the antimicrobial effect. As shown in panels C and D in Figure 3, the highest antibacterial activity was observed in NSQa instead of NSQc previously determined to more potent by the agar methods. The antibacterial activities of NSQb remained to be the lowest.

TEM images (×200 000) for PU/NSQ nanocomposites are shown in Figure 4. The exfoliated NSQa were well dispersed in PU at both 1% (Figure 4A) and 5% (Figure 4B). However, if the fraction of surfactant in NSQa was reduced from 70% to 50% (abbreviated as NSQa-A50), the dispersion of NSQa was significantly affected. As shown in images C and D in Figure 4, NSQa-A50 were intercalated in the polymer matrix at both concentrations (1% and 5%). NSQb and NSQc were stacked and more aggregated in the PU matrix at 1% (Figure 4E, F).

Figure 5 demonstrates AFM diagrams for the surface of PU/NSQ nanocomposites. The phase diagrams that reflected the sensitive phase shift between the soft PU and hard NSP as well as that between the soft and hard segments of PU matrix could provide additional information for the surface characteristics of PU/NSQ. The brightest areas in phase diagrams represented NSP, while the hard segment of PU was brighter than the soft segment. As evident from the phase diagrams, when the concentration of NSQa was equal or higher than 1%, a part of NSQa were exposed on the surface (Figure 5B, bright domains). On the other hand, NSQb or NSQc at the same concentration were not observed on the surface of PU (Figure 5C, D). NSQc appeared to be buried near but under the surface (shadowlike images, each with the shape of a platelet in Figure 5D). The area of NSP neighborhood on the surface of PU/NSQa was further analyzed by 3D phase diagrams and compared with those of the other materials. On the surface of PU, the soft segments (shown as lowland) were surrounded by the continuous hard segment. As each type of NSQ was added into PU, the region of soft segment increased and that of hard segment became discrete. The lateral domain size of PU hard segment on the surface was estimated and ranked as PU/NSQb (~80 nm)> PU/NSQa (~25 nm) > PU/NSQc (~10 nm). In another words, the presence of any NSQ has modified the characteristic size of phase separation in PU.

The quantitative data [maximum height, root-mean-square (rms) roughness, average roughness and mean height] based on AFM images are summarized in Table 1. The surface rms roughness of PU/NSQb 0.01% and PU/NSQc 0.01% in the nanometric scale was similar to that of the pure PU. On the other hand, the surface rms roughness of PU/NSQa 0.01% was lower than that of the pure PU, but increased at higher concentrations of NSQa.

The FESEM images of 1% PU/NSQ nanocomposites are shown in Figure 6A. PU/NSQa and PU had similarly flat surfaces in the micrometric scale, of which the textures could be seen at higher magnification. On the other hand, PU/NSQb and PU/NSQc demonstrated striated surface, but the areas surrounded by the striation were rather smooth (without texture). The EDS analysis showed that only the surface of PU/NSQa had high silicon content, which was attributed to the presence of NSQa on the surface. In the ATR-IR spectra (Figure 6B), the peak location of the C−H bond and N−H bond on the surface of PU was shifted from 2938 to 2917 cm^{-1} and from 3320 to 3301 cm^{-1} respectively, with the addition of 1% NSQa. Specially, a tiny 1635 cm^{-1} peak (C═C of the benzene ring in PU structure) was observed only in PU/NSQa. The water contact angles of these nanocomposites are shown in Figure 6C. All nanocomposites (1%) had a lower contact angle

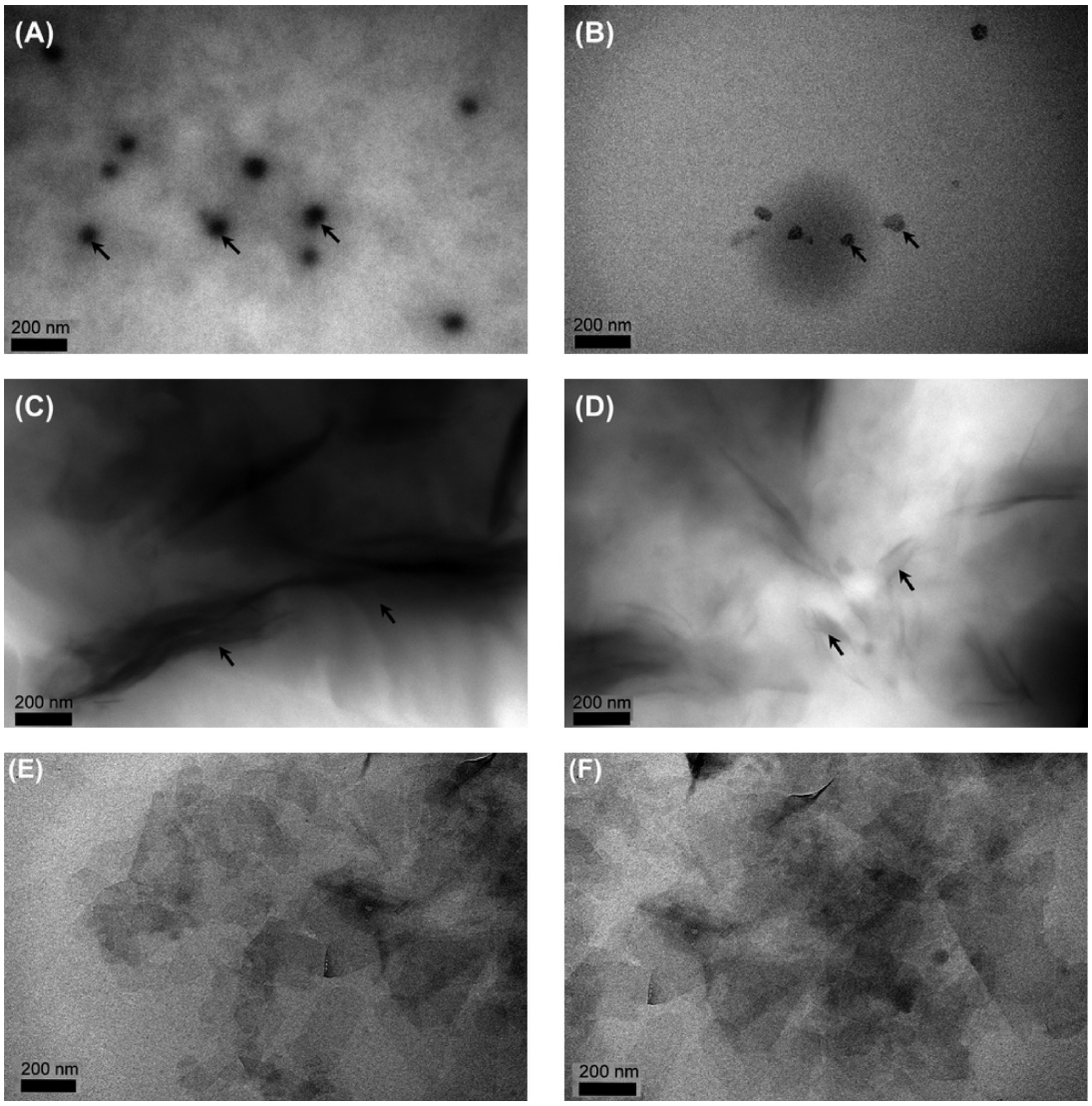

Figure 4. TEM images for PU/NSQa A30 (top) and A50 (bottom) nanocomposites with (A, C) 1% and (B, D) 5% NSQa. Arrows indicate the presence of NSQa in PU matrix. A30 (regular surfactant) and A50 (reduced surfactant) represent that the fraction of surfactant in NSQ was 70% and 50% each. (E, F) TEM images for PU/NSQb 1% and PU/NSQc 1%, respectively.

than the pure PU. Among them, the PU/NSQa had the most dramatic decrease in contact angle (i.e., 95° down to 65°), which also suggested the presence of clay on the surface. The change of surface roughness may be another reason for the different contact angle.

Table 2 shows the results of thermal and mechanical properties of PU/NSQ nanocomposites. When the concentration of NSQa or NSQb in PU increased, the value of T_g also increased. This tendency of change in T_g was opposite to that observed with PU/NSQc. Overall, NSQa increased T_g of the polymer more markedly (from −35.31 to −26.28 °C). As was also expected, the dynamic storage modulus (E') and loss modulus (E'') of PU were enhanced upon the addition of various NSQ. NSQa and NSQb at the higher concentration (1%) did not favor the further change in dynamic modulus, whereas NSQc was just the opposite. The dynamic modulus was the greatest for PU/NSQc 1%.

The static tensile properties of PU and 1% PU/NSQ nanocomposites are summarized in Table 3. The tensile strength of PU/NSQa nanocomposites increased significantly and was 25.1% more than that of PU. The Young's modulus of PU/NSQa and PU/NSQc was also significantly increased (73.4% and 39.5% more, respectively). The elongation of PU simultaneously increased (11.7% more) for PU/NSQa and PU/NSQb. Overall, PU/NSQa nanocomposites had the best mechanical properties among all materials.

The attachment and proliferation of ECs on the surface of PU/NSQ nanocomposites are demonstrated in Figure 7A. At 24 or 72 h, the greatest number of ECs was observed on the surface of PU/NSQa 1%. The number of cells was even larger than that on the control tissue culture polystyrene (TCPS) dish. The nanocomposite PU/NSQc 1% also had a relatively higher cell number at 72 h.

To further elucidate the possible mechanism responsible for enhancement of cytocompatibility in PU/NSQa 1%, Figure 7B compared the attachment and proliferation of ECs on the surface of PU/NSQa (the group marked "A30") and PU/NSQa-A50 as well as PU mixed only with the surfactant Qa (i.e., PU/Qa, where Qa was the fatty amine surfactant in NSQa). High cell viability was demonstrated on the surface of PU/NSQa 1% in both A30 and A50 groups. The addition of pure surfactant in the mixture ("PU/Qa") also increased the

dx.doi.org/10.1021/am2014103 | ACS Appl. Mater. Interfaces 2012, 4, 338−350

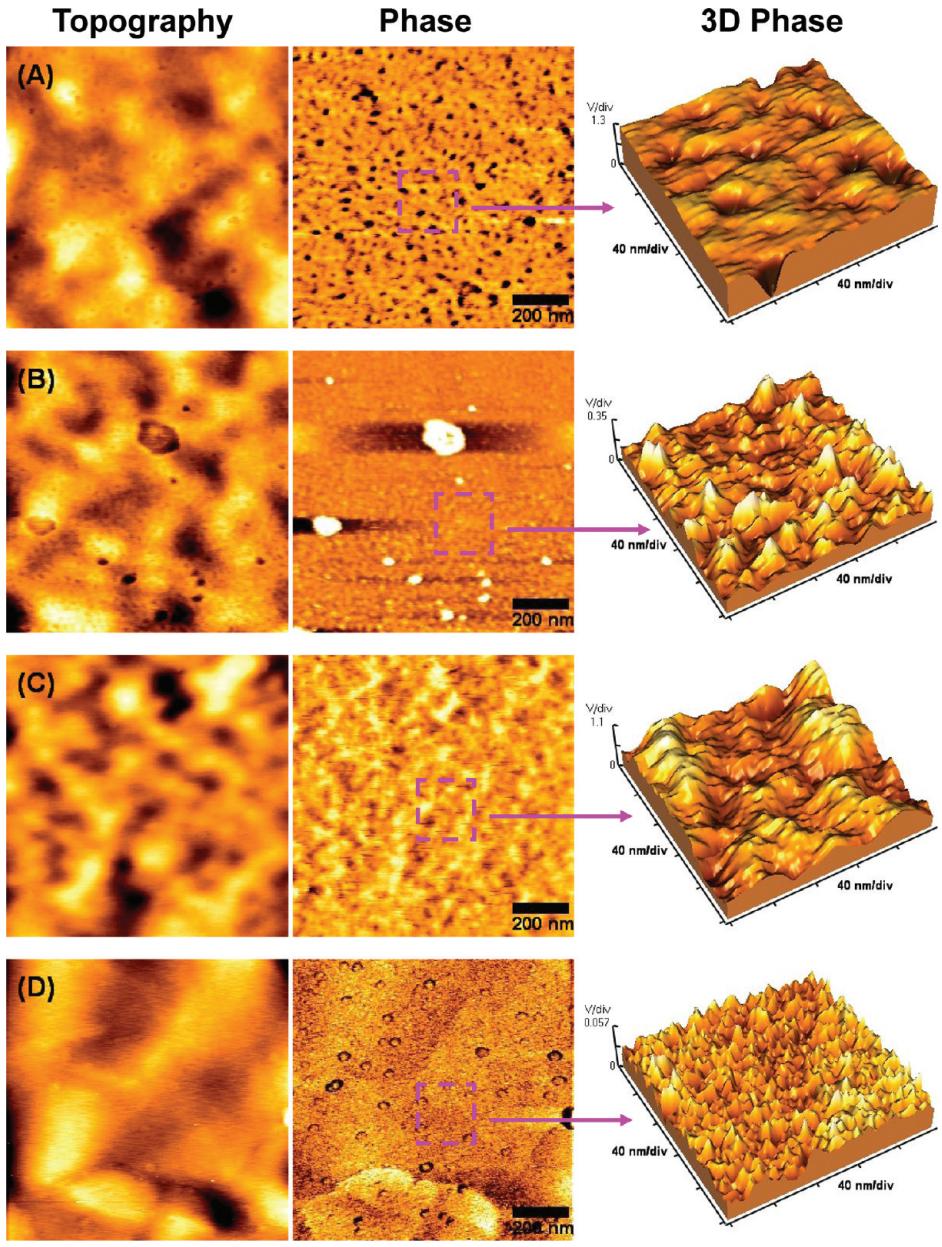

Figure 5. Surface topography (left), phase (middle), and zoom-in 3D phase (right) diagrams of PU/NSQ nanocomposites obtained by AFM. (A) PU, (B) PU/NSQa 1%, (C) PU/NSQb 1%, and (D) PU/NSQc 1%.

Table 1. Surface Topographical Data Based on AFM Images of Different PU/NSQ Nanocomposites

materials		max. height (nm)	root mean square (rms) roughness (nm)	average roughness (nm)	mean height (nm)
pure PU		12.31 ± 2.36	2.30 ± 0.63	1.90 ± 0.55	8.67 ± 0.57
PU/NSQa	0.01%	4.79 ± 0.43	0.87 ± 0.14	0.71 ± 0.13	2.78 ± 0.10
	0.1%	4.52 ± 0.71	0.65 ± 0.14	0.51 ± 0.11	3.52 ± 0.15
	1.0%	6.72 ± 1.36	1.07 ± 0.12	0.86 ± 0.09	5.58 ± 0.15
	5.0%	25.99 ± 5.68	3.12 ± 0.61	2.15 ± 0.37	8.86 ± 0.41
PU/NSQb	0.01%	13.51 ± 3.07	1.86 ± 0.19	1.41 ± 0.09	10.98 ± 0.11
	0.1%	8.46 ± 0.19	1.34 ± 0.01	1.06 ± 0.02	5.03 ± 0.11
	1.0%	8.07 ± 0.54	1.20 ± 0.10	0.94 ± 0.05	4.75 ± 0.03
PU/NSQc	0.01%	15.04 ± 0.33	2.37 ± 0.26	1.90 ± 0.27	9.60 ± 0.22
	0.1%	12.04 ± 2.26	2.18 ± 0.34	1.74 ± 0.27	7.90 ± 0.22
	1.0%	6.42 ± 4.88	0.46 ± 0.03	0.38 ± 0.02	2.60 ± 0.03

cell viability at 72 h, especially at the lower concentration (e.g., PU/Qa 0.1%). Quite surprisingly, increasing the amount of NSQa in PU from 1% to 5% caused a dramatic reduction in cell proliferation (for both A30 and A50). The attachment and proliferation of human skin fibroblasts are further shown in Figure 7C. Regardless of the type of cells, a lower amount of

dx.doi.org/10.1021/am2014103 | ACS Appl. Mater. Interfaces 2012, 4, 338−350

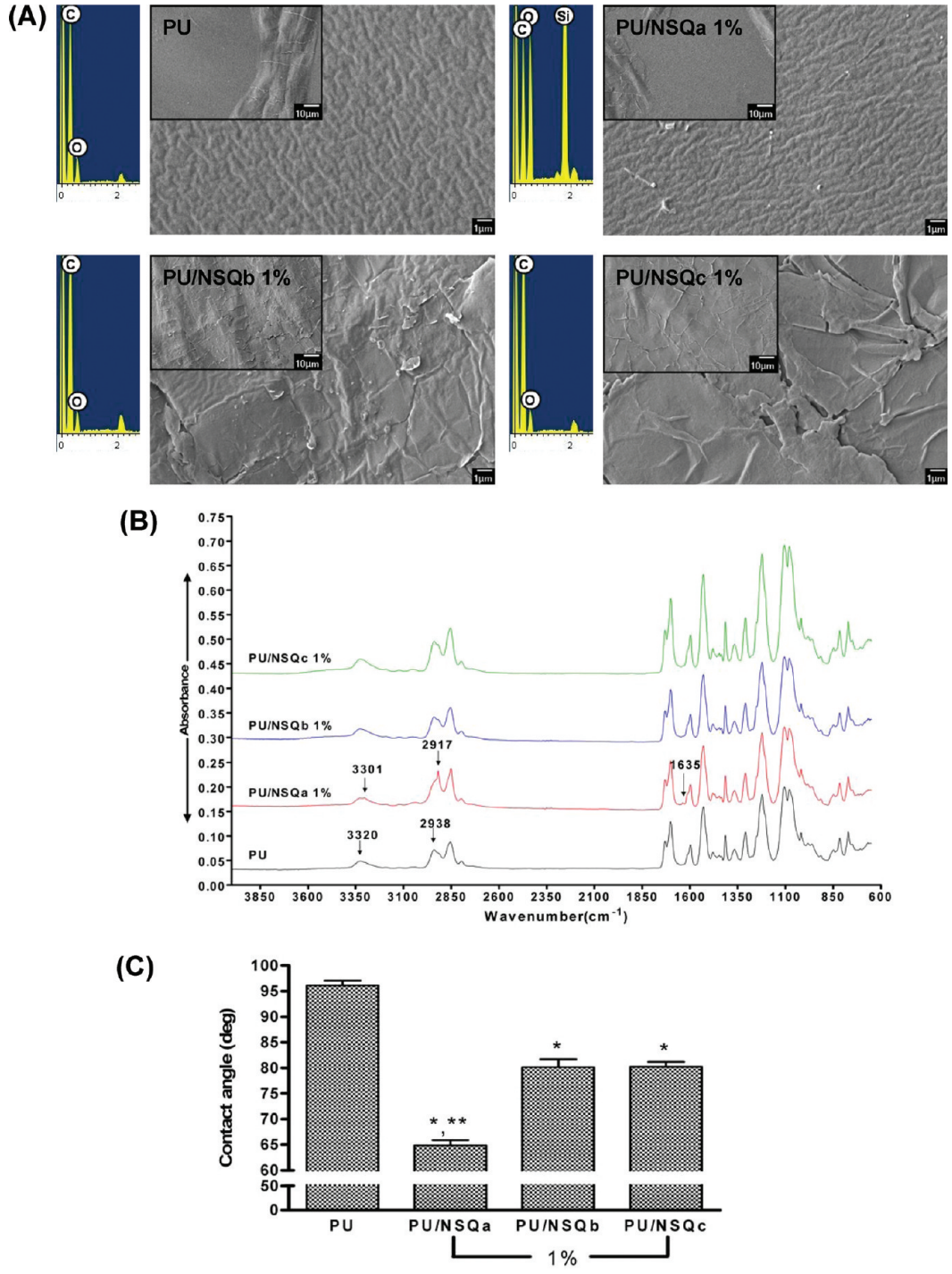

Figure 6. (A) FESEM images (with EDS), (B) ATR-IR spectra (4000−600 cm^{-1}) and (C) The water contact angle of the PU/NSQ nanocomposites (NSQ 1%). *, $p < 0.05$, significantly greater than pure PU. **, $p < 0.05$, significantly greater than all other samples.

cells was consistently observed on the surface of PU/NSQa 5%, especially for the A30 groups.

The microbiostatic effect of PU/NSQ nanocomposites is shown in Figure 8A. As the concentration of NSQ reached 1%, the microbiostasis ratio for all materials reached almost 100% (for standard inoculum). Decreasing the concentration of NSQ from 1% to 0.1% and to 0.01% could help to distinguish the antibacterial activity among various nanocomposites. PU/NSQa nanocomposites showed a dose-dependent microbiostatic effect. They had smaller microbiostasis ratios than the other materials at low NSQa concentrations, but showed strong microbiostatic effect (~100%) at 1% NSQa. Figure 8B showed the microbiostasis ratios of PU/NSQ 1% when the inoculum was increased to 1×10^8 CFU/mL. The microbiostasis ratio was the greatest in PU/NSQc, followed closely by PU/NSQa. Figure 8C showed the microbiostasis ratios for PU/NSQ 1% under the standard inoculum of *E. coli*. The result followed a similar tendency as previously observed for *S. aureus* but the ratios were in general lower.

The biocompatibility of PU/NSQ nanocomposites in vivo is illustrated in Figure 9. The FESEM images (Figure 9A "Without cells") showed many fissures on the surface of PU/NSQb and

dx.doi.org/10.1021/am2014103 | ACS Appl. Mater. Interfaces 2012, 4, 338−350

Table 2. Glass Transition Temperature (T_g) and Dynamic Mechanical Properties of PU and PU/NSQ Nanocomposites

materials		T_g (°C)	E'(MPa) at 37 °C	E''(MPa) at 37 °C	tan δ at 37 °C
pure PU		−35.4 ± 0.05	13.4 ± 0.15	0.9 ± 0.03	0.066 ± 0.003
PU/NSQa	0.01%	−30.7 ± 0.08	19.7 ± 0.22	1.4 ± 0.03	0.070 ± 0.003
	0.1%	−26.3 ± 0.05	17.7 ± 0.27	1.2 ± 0.02	0.068 ± 0.002
	1.0%	−28.4 ± 0.08	12.9 ± 0.19	1.0 ± 0.04	0.081 ± 0.002
PU/NSQb	0.01%	−34.7 ± 0.06	21.1 ± 0.41	1.5 ± 0.05	0.071 ± 0.004
	0.1%	−33.8 ± 0.03	19.8 ± 0.76	1.3 ± 0.02	0.067 ± 0.001
	1.0%	−31.9 ± 0.07	16.4 ± 0.44	1.0 ± 0.04	0.066 ± 0.001
PU/NSQc	0.01%	−34.7 ± 0.06	16.3 ± 0.21	1.1 ± 0.04	0.067 ± 0.002
	0.1%	−36.4 ± 0.07	19.2 ± 0.24	1.4 ± 0.04	0.074 ± 0.001
	1.0%	−36.8 ± 0.06	27.6 ± 0.61	2.1 ± 0.07	0.076 ± 0.001

Table 3. Stress−Strain Behavior of PU and PU/NSQ Nanocomposites

	tensile strength (MPa)	Young's modulus (MPa)	elongation (%)
PU	25.0 ± 9.7	25.0 ± 8.7	311.2 ± 94.4
PU/NSQa 1%	31.3 ± 4.7	43.4 ± 15.4	345.7 ± 21.6
PU/NSQb 1%	27.8 ± 9.0	21.6 ± 4.7	347.9 ± 30.0
PU/NSQc 1%	25.5 ± 5.3	34.9 ± 12.5	325.4 ± 10.3

PU/NSQc nanocomposites. Meanwhile, more pits were observed on PU than on PU/NSQa. Similar surface textures also appeared on all materials covered with cells (Figure 9A "With cells"). The cells on the surface of PU/NSQb and PU/NSQc were larger and more flattened than those on PU/NSQa. The capsule thickness on either the skin or muscle side of PU/NSQb was relatively greater (Figure 9B). The capsule thickness at the muscle side of PU/NSQa or PU/NSQc was much smaller than that of PU. These results demonstrated that PU/NSQa was more biostable and biocompatible than PU alone, whereas another nanocomposite PU/NSQb appeared to be the least biostable and biocompatible.

4. DISCUSSION

Three different surfactants were respectively used to modify the exfoliated clay NSP in this study. The purpose of modification was to enhance the dispersibility of NSP in organic solvents and to form nanocomposites with polymers more readily. Three different kinds of surfactants were used for modifying NSP consisting of sodium counterions and SiO anions. The binding strength between NSP and each surfactant, however, was different because of the different binding nature. For the cationic surfactants, the ionic exchange reaction occurred to form NSQa. For NSQb, the nonionic surfactant could only associate with the SiONa functionalities by a complexation through the −C−C−O− polar interaction in the structure. By using an anionic surfactant, the NSQc was generated by the cation−anion charge pair interaction. The binding strength was thus estimated to rank as NSQa > NSQb ≈ NSQc according to the nature of binding.

The absolute value of zeta potential in general can reflect the stability of particles in solution. As the absolute value of zeta potential is greater than 30 mV, the particles are well dispersed and hardly coagulate in water.[24] The absolute values of zeta potential for both NSP and NSQa were higher than 30 mV, whereas the charge was opposite to each other. As mentioned, Qa was bound to NSP more tightly, which may have helped the dispersion of NSP in solution. On the other hand, the weak binding between NSP and Qb (or Qc) decreased the absolute value of zeta potential to the critical range of coagulation (~30 mV). For the dispersibility reason, the cationic surfactant (Qa) may have been better than nonionic (Qb) and anionic (Qc) ones for surface modification of NSP.

The antibacterial results of various NSQ also revealed the binding strength between NSP and surfactants. Qc has been reported to be an excellent antibacterial and antiviral agent.[25] Due to the weak binding, Qc diffused more easily in agar, and the antibacterial ability of NSQc obtained from the agar diffusion and halo zone methods (both using agar) was significantly greater than that observed for NSQa and NSQb. On the other hand, the evaluation of antibacterial activities by the direct contact method showed that NSQc had a lower antimicrobial effect, in which case the concentration of Qc was diluted by the solution used in the method. For NSQa, the positive charge on the surface may have caused the bacteria (negatively charged) to be quickly covered, which interfered with the nutrient transport from the broth,[9] and led to the higher antibacterial activity. On the basis of the fact that the diffusion of nanomaterials may be slow, the direct contact method should be more appropriate than the other two protocols to assess the antibacterial activity of such nanomaterials. No matter what protocol was used, all NSQ showed better antibacterial effect than the unmodified NSP. In spite of being highly antimicrobial, NSQ showed lower cytotoxicity compared with NSP. Capping by surfactants may reduce the direct exposure of nanomaterials and the related damage to mammalian cell membrane.[11] Taken together, these results suggested that surfactant-stabilized NSP may be safer and simultaneously more antimicrobial, than the original NSP.

TEM images demonstrated that when NSQ and polymer were mixed into nanocomposites, the surfactant to NSP ratio affected the dispersibility of NSQ in the polymer matrix. A higher ratio of the surfactant to NSP (e.g., as in A30) could better maintain the exfoliation state of NSP. Since the mass of exfoliated clay needed to reach the same mechanical property was usually lower than that of intercalated clay in a polymer matrix,[5] a higher surfactant to NSP ratio may be more advantageous.

Results from PU composites containing different modified clays also revealed the significantly different distribution and contribution of these clays in a polymer. The surface topography of PU/NSQa nanocomposites was very different from that of PU/NSQb or PU/NSQc nanocomposites based on SEM as well as AFM images. The average height and rms roughness of PU/NSQa surface were reduced, while those of PU/NSQb or PU/NSQc surface remained similar to the pure PU. Only PU/NSQa but not other nanocomposites showed a small difference in ATR-IR spectra from that of PU. The water

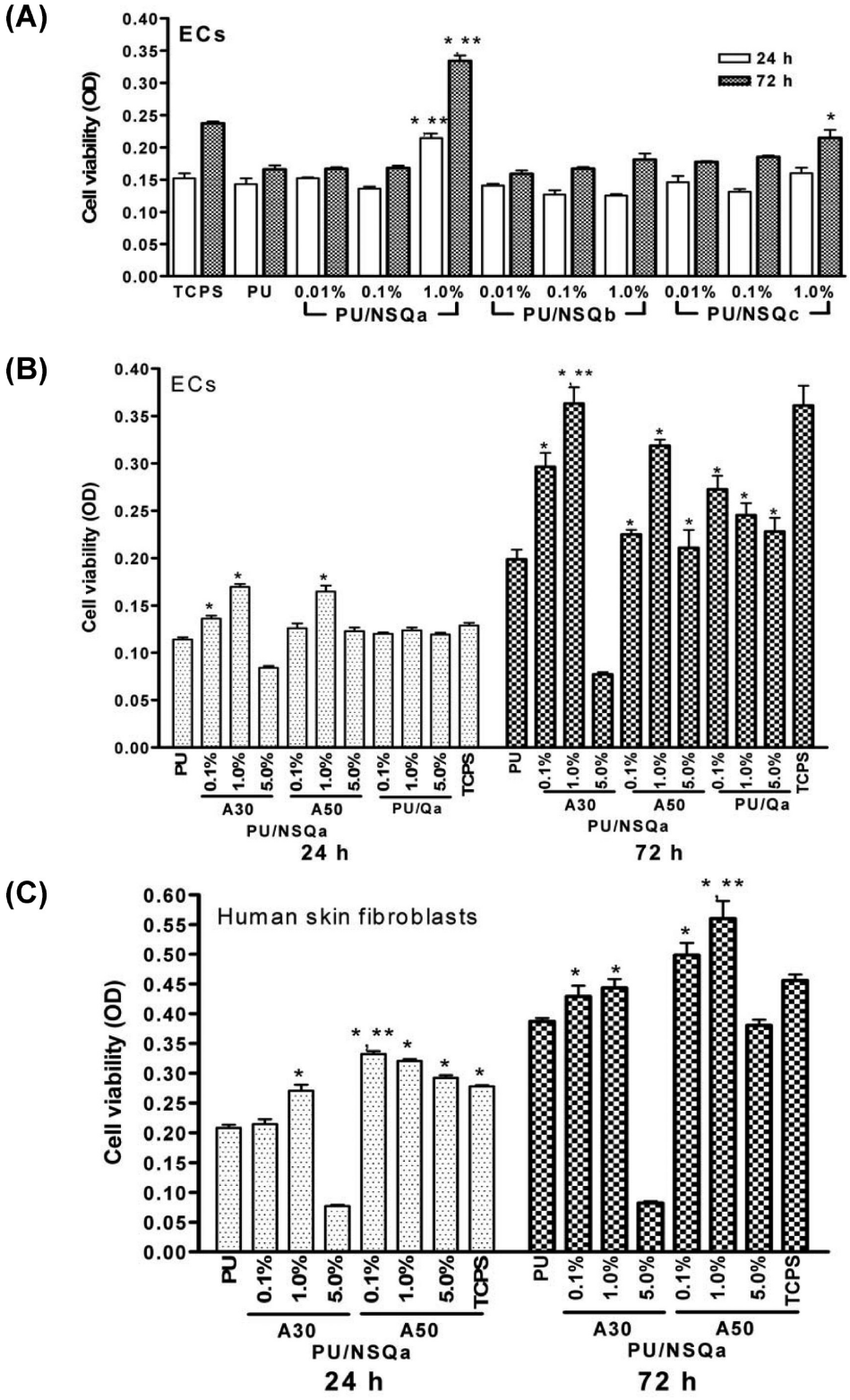

Figure 7. (A) Viability of endothelial cells (ECs) grown on the surface of PU/NSQ nanocomposites at 1 and 3 days. *: $p < 0.05$, significantly greater than pure PU. **, $p < 0.05$, significantly greater than all other samples. BB) The viability of ECs grown on the surface of PU/NSQa (A30 and A50) and PU/Qa nanocomposites at 1 and 3 days. *, $p < 0.05$, significantly greater than pure PU. **, $p < 0.05$, significantly greater than all other samples. (C) The viability of human skin fibroblasts grown on the surface of PU/NSQ nanocomposites at 1 and 3 days. *, $p < 0.05$, significantly greater than pure PU. **, $p < 0.05$, significantly greater than all other samples.

contact angle of PU/NSQa decreased significantly from 95 to 65°. These results suggested that only NSQa may have been exposed to the surface of PU by a stronger interaction between them and PU chains, which gave rise to distinct surface properties of PU/NSQa nanocomposites. Nanomaterials in high concentrations usually form aggregates in polymers, which decreased the thermal or mechanical properties of nanocomposites.[2] Moreover, NSP undergo self-assembly and are thus

dx.doi.org/10.1021/am2014103 | ACS Appl. Mater. Interfaces 2012, 4, 338–350

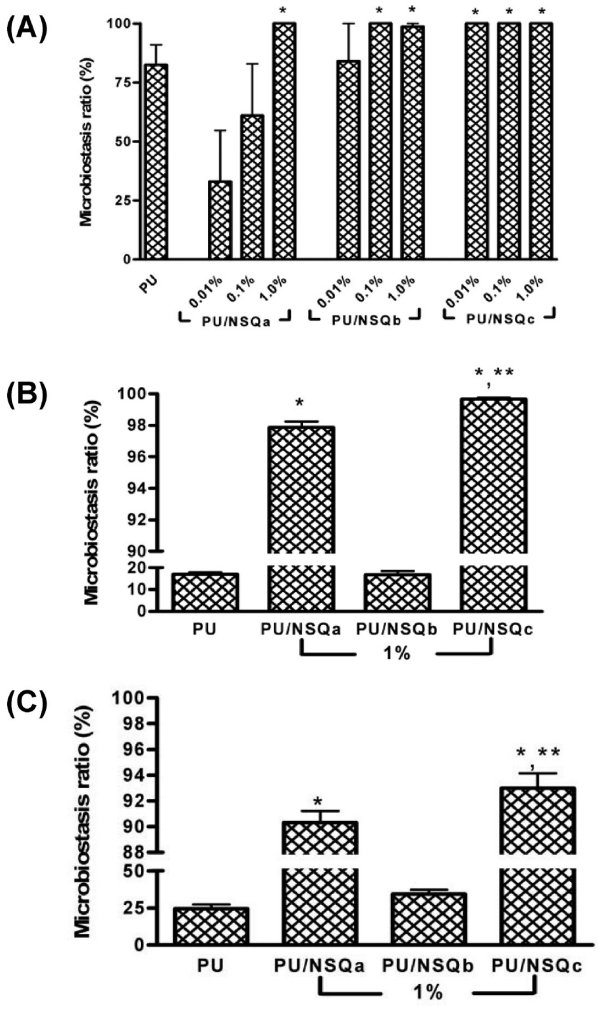

Figure 8. Microbiostasis ratios of PU/NSQ nanocomposites inoculated with (A) 1×10^6 CFU/mL (standard inoculum) and (B) 1×10^8 CFU/ml (increased inoculum) of *S. aureus* as well as (C) 1×10^6 CFU/ml of *E. coli*, evaluated at 24 h by JIS Z2801.

difficult to be dispersed at high concentrations while maintaining their exfoliation state in a polymer. Therefore, an adequate ratio of clay to surfactant is necessary.

Polymer/clay nanocomposites often increase the heat resistance and mechanical property.[5] The T_g value of PU/NSQa nanocomposites was higher than that of the other materials. Again, the binding strength between NSP and surfactants appeared to affect the dispersion of clay in the polymer and change the polymer properties accordingly. The increase in Young's modulus and tensile strength of PU/NSQ nanocomposites also revealed a similar tendency to the increase in thermal properties.

ECs, the cells lining the blood vessels, exhibited fast attachment (24 h) and proliferation (72 h) on the surface of the PU/NSQa 1% nanocomposite. This promoting effect was outstanding because the numbers of cells on the mentioned nanocomposite were even higher than those on the TCPS cell culture dish. As mentioned, some NSQa may have moved to the surface of PU. The silicate component in NSQa may have modified the cellular response of PU. Calcium silicate has been reported to be biocompatible and to possess bioactivity.[26] It was thus likely that NSQa may enhance cellular attachment and proliferation when exposed on the PU surface. In addition,

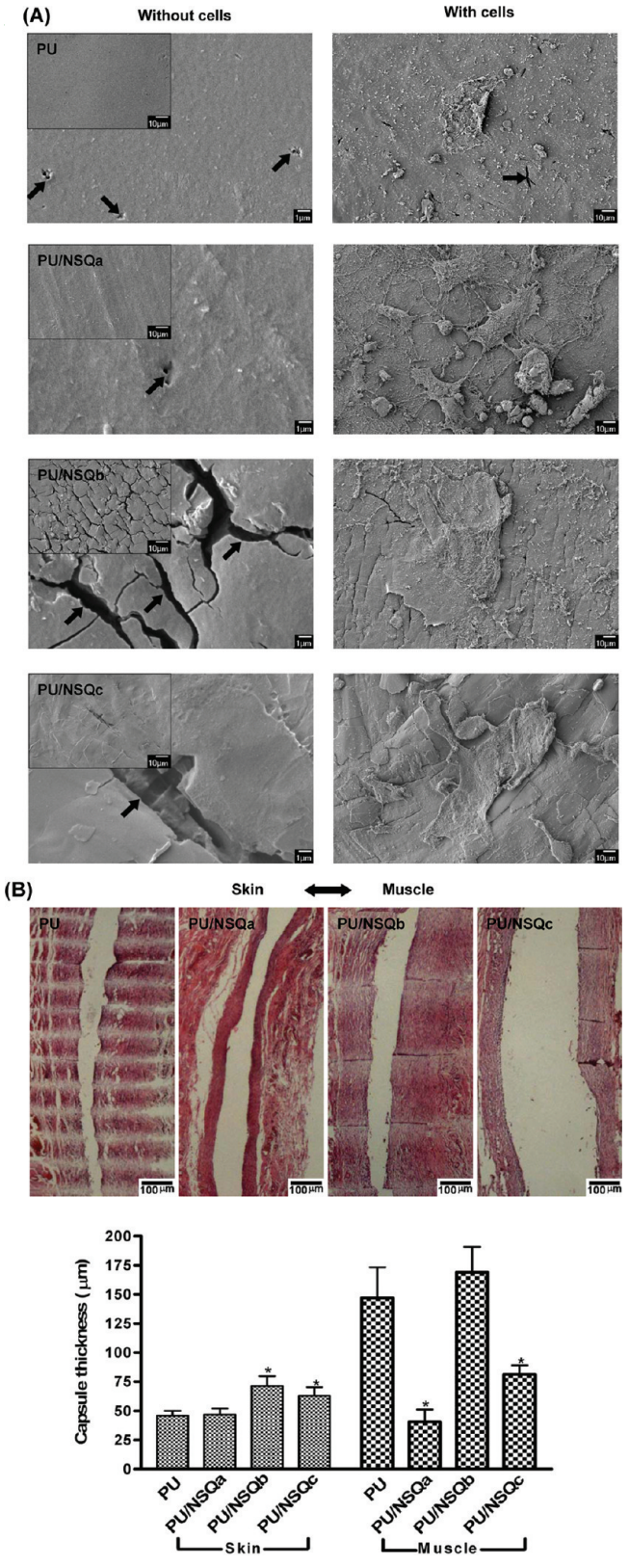

Figure 9. (A) FESEM images for the surface of PU/NSQ 1% nanocomposites in vivo with cells and without cells (cleansed surfaces). (B) The images showing the foreign body capsules surrounding each material (on the skin side and muscle side), and quantification of the capsule thickness for PU/NSQ 1% nanocomposites in vivo. *, $p < 0.05$, significantly greater or lower than PU.

NSQa modified the hard domain size of PU to ~25 nm, which was in the range for nanopattern-enhanced cell attachment

dx.doi.org/10.1021/am2014103 | ACS Appl. Mater. Interfaces 2012, 4, 338–350

and proliferation.[27,28] On the other hand, PU containing the cationic surfactant Qa only (without NSP) did not have such a remarkable effect especially in cell attachment. Therefore, the nanomaterials may more efficiently modify the surface of PU than the molecules. But as the concentration of NSQa-A30 in PU increased to 5%, a dramatic reduction in cell proliferation was found in all types of cells. Therefore, NSQa in an excess amount on the surface of PU may eventually inhibit the cellular attachment and proliferation. In another words, by controlling the concentration of NSQa in PU, the PU/NSQa nanocomposites can be designed to either enhance or inhibit the cell attachment for different biomedical applications. The sudden loss of cell affinity in the presence of 5% NSQa was an interesting phenomenon. We suspected that this nonadherence feature may be associated with the high contact angle (~96.4°) initially and the excessive surface hydration later which was brought about by the silicates in the polymer.[29] The actual mechanism should require further investigation.

All PU/NSQ nanocomposites showed antimicrobial effects. The microbiostasis ratio reached 100% for all materials containing 1% NSQ inoculated with a regular amount of microbes. Because Qc may be released from the PU/NSQc nanocomposite as mentioned, the antibacterial activity of PU/NSQc 0.01% was very high even for an increased amount of microbial inoculum. However, Qc was suspected to cause cancer[30] and was suggested to be used in only toothpastes, shampoos and shaving foams on skin in low concentrations. Therefore, the biomedical safety of PU/NSQa should be better than that of PU/NSQc.

PU/NSQa 1% showed thinner fibrous capsules in rat implantation. This result was parallel to the FESEM observation. The biocompatibility of PU is usually associated with the biostability and surface integrity.[31] The addition of NSQa improved the biocompatibility of PU probably due to the modification of surface nanostructure by the presence of NSQa. Because PU/NSQa evoked less foreign body reaction, its surface integrity also remained better than the other materials after implantation for a period of time in vivo.

Organic compounds, such as chlorhexidine diacetate and quaternary ammonium, usually have cytotoxicity and health concerns when they are intended to be used in vivo. These organic compounds were used to modify clays and to mix them in PU and other polymers in about 5%.[17,18] Because of high concentration and poor dispersion of these organically modified clays in polymer, these polymeric nanocomposites exhibited excellent antimicrobial activity but inferior biocompatibility. The low concentration (1%) of exfoliated NSQa in PU in this study successfully improved the biocompatibility and maintained the antimicrobial activity at the same time. Besides, all NSQ in this study has been analyzed by dialysis. The free surfactants were not detected in NSQa or NAQb and only a limited amount (<20%) of surfactant was observed in NSQc. The results from dialyzed NSQ were not significantly different from those obtained using undialyzed NSQ, suggesting that the role of leachable surfactants may be relatively minor.

In summary, NSQa in PU tended to move to the surface and modified the surface of PU. This phenomenon was less evident in the case of NSQb and NSQc. The PU/NSQa 1% nanocomposite demonstrated the greatest antimicrobial activity and biocompatibility. By choosing a proper surfactant to cap the delaminated clay, it is possible to develop PU nanocomposites that contain a small amount of clay but have significant improvement in the medical and biological performances.

5. CONCLUSION

In this study, we investigated and demonstrated the physical properties, antimicrobial activity, and biocompatibility of the exfoliated clay NSP, three types of surfactant-modified NSP (NSQ), and the nanocomposites made from PU and NSQ. Unlike NSP, none of the NSQ exhibited cytotoxicity at low concentration. NSQ modified by the cationic or anionic surfactant (NSQa or NSQc) displayed excellent antimicrobial activity at 1% concentration. The addition of 1% NSQa in PU matrix was found to increase the tensile properties and modify the surface morphology of PU, which enhanced the attachment and proliferation of cells, reduced the foreign body reaction, and inhibited the growth of bacteria. PU/NSQa nanocomposites with favorable biocompatibility and antimicrobial activity may have potential biomedical applications.

AUTHOR INFORMATION

Corresponding Author

*E-mail: shhsu@ntu.edu.tw.

ACKNOWLEDGMENTS

This study was supported by grants from the National Science Council, Taiwan (Grant NSC100-2120-M-002-006).

REFERENCES

(1) Hsu, S. H.; Tang, C. M.; Tseng, H. J. *Acta Biomater.* **2008**, *4*, 1797.
(2) Hsu, S. H.; Tang, C. M.; Tseng, H. J. *Biomacromolecules* **2008**, *9*, 241.
(3) Wang, S. F.; Shen, L.; Tong, Y. J.; Chen, L.; Phang, I. Y.; Lim, P. Q.; Liu, T. X. *Polym. Degrad. Stab.* **2005**, *90*, 123.
(4) Alexandre, M.; Dubois, P. *J. Mater. Sci. Eng., R* **2000**, *28*, 63.
(5) Sinha Ray, S.; Okamoto, M. *Pro. Polym. Sci.* **2003**, *28*, 1539.
(6) Chou, C.-C.; Lin, J.-J. *Macromolecules* **2004**, *38*, 230.
(7) Chu, C.-C.; Chiang, M.-L.; Tsai, C.-M.; Lin, J.-J. *Macromolecules* **2005**, *38*, 6240.
(8) Lin, J.-J.; Chu, C.-C.; Chiang, M.-L.; Tsai, W.-C. *J. Phys. Chem. B* **2006**, *110*, 18115.
(9) Hsu, S. H.; Tseng, H. J.; Hung, H. S.; Wang, M. C.; Hung, C. H.; Li, P. R.; Lin, J. J. *ACS Appl. Mater. Interfaces* **2009**, *1*, 2556.
(10) Lin, J. J.; Chu, C. C.; Chiang, M. L.; Tsai, W. C. *Adv. Mater.* **2006**, *18*, 3248.
(11) Teow, Y.; Asharani, P. V.; Hande, M. P.; Valiyaveettil, S. *Chem. Commun.* **2011**.
(12) Lamba, N. M. K.; Woodhouse, K. A.; Cooper, S. L. *Polyurethane in Biomedical Application*; CRC Press: Boca Raton, 1998.
(13) Ajili, S. H.; Ebrahimi, N. G.; Soleimani, M. *Acta Biomater.* **2009**, *5*, 1519.
(14) Moraes, C.; Kagoma, Y. K.; Beca, B. M.; Tonelli-Zasarsky, R. L.; Sun, Y.; Simmons, C. A. *Biomaterials* **2009**, *30*, 5241.
(15) Jung, I. K.; Bae, J. W.; Choi, W. S.; Choi, J. H.; Park, K. D. *J Biomater. Sci. Polym. Ed.* **2009**, *20*, 1473.
(16) Hsu, S. H.; Kao, Y. C. *Macromol. Biosci.* **2004**, *4*, 891.
(17) Poolewarren, L.; Farrugia, B.; Fong, N.; Hume, E.; Simmons, A. *Appl. Surf. Sci.* **2008**, *255*, 519.
(18) Styan, K. E.; Martin, D. J.; Poole-Warren, L. A. *J. Biomed. Mater. Res. Part A* **2008**, *86A*, 571.
(19) Nigmatullin, R.; Gao, F.; Konovalova, V. *Macromol. Mater. and Eng.* **2009**, *294*, 795.
(20) Nigmatullin, R.; Gao, F.; Konovalova, V. *J. Mater. Sci.* **2008**, *43*, 5728.
(21) Lin, J.-J.; Chen, Y.-M. *Langmuir* **2004**, *20*, 4261.
(22) Lai, Y.-H.; Chiu, C.-W.; Chen, J.-G.; Wang, C.-C.; Lin, J.-J.; Lin, K.-F.; Ho, K.-C. *Sol. Energy Mater. Sol. Cells* **2009**, *93*, 1860.
(23) Rojo, L.; Barcenilla, J. M.; Vazquez, B.; Gonzalez, R.; San Roman, J. *Biomacromolecules* **2008**, *9*, 2530.

(24) Benefield, L. D.; Judkins, J., Joseph, F.; Weand, B. L. *Process Chemistry for Water and Wastewater Treatment*; Prentice-Hall: Englewood Cliffs, NJ, 1982.
(25) Piret, J.; Lamontagne, J.; Bestman-Smith, J.; Roy, S.; Gourde, P.; Desormeaux, A.; Omar, R. F.; Juhasz, J.; Bergeron, M. G. *J. Clin. Microbiol.* **2000**, *38*, 110.
(26) Ding, S.-J.; Shie, M.-Y.; Hoshiba, T.; Kawazoe, N.; Chen, G.; Chang, H.-C. *Tissue Eng. Part A.* **2010**, *16*, 2343.
(27) Dalby, M. *Exp. Cell Res.* **2002**, *276*, 1.
(28) Dalby, M. J.; Giannaras, D.; Riehle, M. O.; Gadegaard, N.; Affrossman, S.; Curtis, A. S. G. *Biomaterials* **2004**, *25*, 77.
(29) Sinha Ray, S.; Yamada, K.; Okamoto, M.; Ueda, K. *Nano Lett.* **2002**, *2*, 1093.
(30) Decker, H.; Ryan, M.; Jaenicke, E.; Terwilliger, N. *J. Biol. Chem.* **2001**, *276*, 17796.
(31) Christenson, E. M.; Anderson, J. M.; Hiltner, A. *J.Biomed. Mater. Res., Part A* **2004**, *70A*, 245.